Measuring and modelling nearshore recovery of an eroded beach in Lake Michigan, USA.

Chelsea A. Volpano[a,*], Lucas K. Zoet[a], J. Elmo Rawling III[b], E.J Theuerkauf[c]

[a]Department of Geoscience, University of Wisconsin Madison, 1215 West Dayton Street, Madison, WI, 53703, USA.

[b]Wisconsin Geological and Natural History Survey, University of Wisconsin Madison, 3817 Mineral Point Road, Madison, WI 53705, USA.

[c]Department of Geography, Michigan State University, Geography Building,

673 Auditorium Rd, East Lansing, MI 48824, USA.

*Corresponding author: cvolpano@wisc.edu

Abstract

Erosion by storms and high-water levels impacts large enclosed basins; however there have been few attempts to numerically model cumulative impacts in large lakes. Antecedent morphology is a large determinant of coastal sensitivity to storms, so capturing the beach recovery is important for overall vulnerability assessment. To study beach recovery, we apply the numerical model XBeach to simulate a period of low to moderate wave energy when beach recovery typically occurs. Surveys were conducted one month apart during summer of 2020 on the west coast of Lake Michigan and used to initiate model runs and evaluate model performance. XBeach was used to propagate offshore wave conditions from a Great Lakes Coastal Forecasting System (GLCFS) node ~1 km offshore into the nearshore, and results were compared to measurements from a nearshore pressure sensor. We tested for the optimal value of the asymmetry/skewness parameter (*facua*) for model-data convergence. We evaluated model skill using a Mean Square Error Skill Score (MSESS) and a decomposition. In our repeat surveys we observed slight landward migration of longshore bars and the initiation of bar welding to the shoreline but, overall, changes in bathymetry were small. We found that XBeach transforms offshore waves well and sediment transport volume was accurately predicted by the model. However, XBeach did not capture the morphologic evolution under low energy conditions, preventing simulation of beach recovery. Overall, higher values of *facua* resulted in improved skill scores and modeled nearshore morphology that was more similar to the morphology measured in our surveys.

Keywords: XBeach; Great Lakes; Coastal Erosion; Beach Recovery; Sediment Transport

Introduction

Numerical modelling is well developed and implemented for a range of geomorphic applications on marine coasts but is rarely applied in the North American Great Lakes (NAGL). Numerical models can simulate impacts of storms (Barnard et al., 2014; 2019), sea-level rise (Barnard et al., 2019; Ranasinghe, 2016), and flooding (Roelvink et al., 2009) on coastal evolution. Regional models integrate sediment supply to the nearshore with longshore transport to predict shoreline changes over many spatial and temporal scales (e.g., Bamunawala et al., 2020; Roelvink et al., 1999; Sherwood et al., 2000; 2002; Warner et al., 2008). In the NAGL, periodic high-water levels can generate vulnerable coastal morphology (Theuerkauf et al., 2021) that exacerbates rates of coastal erosion caused by storm driven wave runup (e.g, Baird, 2010; Davidson-Arnott, 1989; 2010; Meadows et al., 1997; Braun and Theuerkauf, 2021). Recent accelerated erosion (Krueger et al., 2020; Roland et al., 2021; Volpano et al., 2020) is revealing that coastal management tools (e.g., accurate sediment transport and morphological modelling) are lacking for the NAGL, but their development could help define combinations of storm and lake level conditions that would be most detrimental to coastal sites. This would better inform coastal managers on the timing and extent of threats to shoreline property and infrastructure, particularly as the focus in the NAGL shifts to coastal resilience and sustainable management (Gallagher et al., 2020; Lake Huron Centre for Coastal Conservation, 2019; GLCRI, 2018).

Many of the coastal processes operating in the NAGL are similar to many marine coasts. While storm severity, presence of longshore bars, and the range of nearshore slopes are comparable (Cavaleri, 2018, Davidson-Arnott, 1988, Davis et al., 1972; Hands, 1979; 1984), several hydrodynamic parameters are unique to the NAGL. Limited fetch conditions translate to shorter wave periods (Cavaleri, 2018), shore-fast ice is a significant geomorphic agent (Cavaleri, 2018), and water level fluctuations occur over seasonal to decadal timescales (Fry et al., 2020; Gronewold et al., 2021). The smaller scale of enclosed basins leads to larger variability in wind direction, and waves in shallow nearshore waters are subject to bottom effects from small changes in bathymetry and environmental conditions that impact sediment transport (Cavaleri, 2018). Additionally, fluctuations in water level on seasonal, annual, and decadal timescales force NAGL shorelines to constantly adjust towards a dynamic equilibrium condition (Theuerkauf et al., 2021; Volpano et al., 2020).

Fluctuating water levels confound the cycle of erosion and recovery on NAGL beaches. Theuerkauf et al. (2021) found that beach response to major storms is largely influenced by antecedent morphology, which is established through beach recovery in response to prior lake levels and minor storm events. They noted that spring storms, in conjunction with elevated water levels during the summer, prevented beach recovery, exacerbating the impacts of storms during the more energetic wave conditions in fall. Shoreline evolution during high lake level is variable, e.g., transgressing due to increased sediment supply (Davidson-Arnott, 1989) or regressing due to increased wave action (Mattheus 2014; 2016). Beach response can be heavily impacted by littoral sand supplies and thus relate to dynamics impacting the upstream (Mattheus et al., 2017). Predicting how a segment of the coast will respond to changes in lake level or large storms requires knowledge of how sediment moves within the nearshore during low-wave-amplitude recovery periods.

Observational studies of nearshore processes on sandy NAGL shorelines show a strong correlation between coastal erosion and storms (Brown et al., 2005; Davis and Fox, 1972; 1976; Swenson et al., 2006; Theuerkauf et al., 2021, Volpano et al., 2020), elevated lake levels (Davidson-Arnott and van Heyningen, 2003; DuBois, 1973), and structures that interrupt longshore transport (Mattheus, 2019; Morang et al., 2019; Shabica et al., 2011). Morang et al. (2011) suggests that studying shorelines regionally as part of the littoral system is necessary for successful sand management. However, typical transect based monitoring (*e.g*., Emery, 1961) is time consuming and resulting data is limited in representing alongshore variability (Theuerkauf and Rodriguez, 2012). New methods such as small unoccupied aerial systems (sUAS) and topobathy LIDAR increase the spatial and temporal resolution of coastal monitoring and are applied to NAGL shorelines (Reif et al., 2013; Theuerkauf and Braun, 2021; Volpano et al., 2020). Past studies attempt to quantify coastal erosion, littoral transport, and determine the impact of fluctuating water levels in the NAGL (Baird, 2010; Chrzastowski et al., 1994; Dibajnia et al., 2004; Morang et al., 2011; 2019; and references therein). These sediment budget and nearshore transport estimates aim to address limitations of site-specific observations. However, they lack predictive capabilities because they aggregate changes over multiple storm seasons and lake levels, obscuring the individual conditions resulting in sediment transport.

Strong storms are common in the NAGL during the fall and winter (November to April; Angel and Isard, 1998), concurrent with seasonal low water level (Figure 1). High energy wave conditions during these periods increase sediment transport (Davidson-Arnott, 2010; Hands, 1984; Plant et al., 1999) and storms coincident with elevated lake level may significantly impact the nearshore because its morphology cannot effectively dissipate wave energy (Davidson-Arnott, 2010; Houser and Greenwood, 2005; 2007; Theuerkauf et al., 2021). Additionally, the seasonal rise in water levels beginning in spring and peaking in late summer may prevent beach recovery, exacerbating vulnerabilities during subsequent storms (Theuerkauf et al., 2021). The compounding effects of lake level fluctuations and storms complicates sediment transport in the NAGL. The magnitude of a storm that will result in significant sediment transport as well as the impact of stormy intervals relative to quiescent periods depends on the beach profile established during beach recovery. Therefore, the interplay of antecedent morphology and variable coastal processes suggests that estimating beach evolution requires high resolution spatiotemporal observation and modeling efforts to resolve coastal change during these recovery periods.

A range of modeling approaches have been used to simulate coastal change in the NAGL. Early modelling applications in the NAGL applied a combination of deterministic-probabilistic modelling (Davis and Fox, 1976; Fox and Davis, 1973b) based on empirical relationships rather than predictive hydrodynamic physics. Another approach reconstructed patterns of wave diffraction and deflection to estimate hydrodynamic parameters and sediment transport (Booth et al., 1994). They determined that change to the shoreline due to erosion of the outer nearshore is slow and episodic. Recent efforts applied the process based numerical model COSMOS (Nairn and Southgate, 1993) to simulate coastal processes in the NAGL (Baird 2008; Nairn and Zuzek, 2005). Dibajnia et al. (2004) developed a sediment budget for a NAGL harbor and modelled rates of sediment bypass, which were higher during low water conditions. Most recently, Li (2021) used a coupled wave, hydrodynamic and sediment transport model to investigate longshore transport of sediment with lake level fluctuations. They found good agreement between model predictions and observations that net movement of dredged material placed within the nearshore was highest in the cross-shore direction during low wave conditions. These site-specific numerical modelling applications are useful; however, they do not simulate regional three dimensional hydrodynamic processes needed to simulate beach recovery.

A first step in regional nearshore modelling of the NAGL is to develop a scalable workflow to implement process-based numerical models. Here, we examine nearshore sediment transport through a combined field work and modeling approach to test the performance of the hydrodynamic model XBeach during low wave conditions typical of the early summer on a sandy Lake Michigan beach during the record high lake levels of 2020 in order to test the model's capability to predict beach recovery. These quiescent conditions should induce beach recovery and onshore bar movement, but the impact of elevated water levels on this recovery process is not clear. First, we collect repeat high-resolution topography and bathymetry data to measure change and initialize the nearshore hydrodynamic model XBeach. We also characterize the wave climate with wave pressure sensors and used these in situ data to validate the modelling predictions for the transformation of offshore waves from the Great Lakes Coastal Forecasting System (GLCFS) into the nearshore by XBeach. Finally, the modelling results are compared to the measured change to determine how accurately XBeach simulates nearshore morphologic evolution during a period of elevated lake levels and low wave conditions. This step is essential in a modelling workflow documenting coastal erosion because of the compounding effect of potentially limited beach recovery due to high lake levels and seasonal storminess. Without successful predictions of beach recovery processes, it is not possible to accurately quantify the impacts of future storms on coastal erosion.

Study Site

Point Beach is a sandy headland on the western shore of Lake Michigan (Figure 2). The 14-km stretch of beach is backed by a relict strandplain capped by dunes (Figure 2B; Dott and Mickelson, 1995; Mickelson and Socha, 2017). The location of this study (44°12'43.9"N 87°30'27.5"W) is at the approximate inflection point of the gradually curving shoreline (Figure 2). The nearshore is characterized by three quasi-permanent nearshore bars and transient swash bars (Figure 2B). The averaged bathymetric gradient offshore of Point Beach to a depth of 30 m is shallow, between 0.0055-0.0095, and is classified as dissipative according to the Irribarren number (Wright and Short, 1984).

The wave climate at Point Beach is dominated by wind generated waves with the most significant energy inputs from easterly, southeasterly, and northeasterly winds. Fetch is greatest to the southeast. Mean significant wave height at the site for 2020 was 0.6 m, with wave periods of 3 seconds, with a maximum of ~3.7 m and 7.8 sec during large storms (NOAA-GLERL 2020). During our study period (August-September), Point Beach experienced wave conditions lower than typical for 2020 (Figure 3) with a mean significant wave height of 0.4 m and very few waves exceeded 1 m.

There is no significant tidal influence in Lake Michigan, although short term locally elevated water levels of up to 1 m can result from basin-scale water oscillations (seiches) related to storm procession (As-Salek and Schwab, 2002). Seasonal level fluctuations are ±0.3 to 0.4 m (Davidson-Arnott, 1988; Thompson and Baedke 1995; Quinn 2002) and longer-term lake level fluctuations of ±1 m can occur within a decade (Hands, 1984; Sellinger et al., 2008). Record high water levels were reached each month between January and August of 2020, meaning our survey period captured conditions that could limit recovery, i.e., high lake levels and low-moderate wave energy.

Methods

To measure and model nearshore sediment transport, we used survey techniques that allowed rapid acquisition of topo-bathymetric data using drones and a small research vessel. Beach topography, nearshore bathymetry, and wave conditions were measured in two surveys, approximately a month apart (on 08/11/2020 and 09/05/2020). These data were then used to measure nearshore change, and to drive, and subsequently validate, a hindcast model to determine if XBeach could simulate nearshore evolution under record high lake levels and low-moderate wave conditions.

Data Collection

Digital Elevation Model

The subaerial digital elevation model (DEM) was created using structure-from-motion photogrammetry (SfM) using photographs taken from multiple angles (Westoby et al., 2012). Aerial imagery was acquired with a DJI Phantom 4 RTK (Real-time Kinematic) sUAS (small Uncrewed Aerial System; i.e. a drone) that flew autonomously along pre-programmed flight paths created with the MapPilot program. This ensured sufficient image overlap for a given ground sampling distance, which was set at 2.1 cm. The open-source program RTKLIB (ver. 2.4.3 b33; Takasu, 2018) was used to execute Post-Processed Kinematic (PPK) algorithms to provide precise positioning of the acquired photos. The GPS tagged images were adjusted for time and gimbal offsets according to the Aerotas Phantom 4 RTK PPK Processing Workflow (Aerotas, 2018).

Agisoft Metashape was used to align the photographs and create point clouds that were then converted into DEMs (Photoscan, 2018). Ground Control Points (GCPs) were identified in the photographs and post-processed GPS coordinates were used to assess the location-accuracy of the terrain model, described below. A dense point cloud was constructed, and points identified to be noise or high vegetation were removed using LAStools (Isenburg, 2014). A 10 cm resolution DEM was created from the point cloud in ESRI ArcMap 10.4.1 geospatial processing software using the “LAS Dataset to Raster” tool in the LAS Dataset toolbox which calculated the value for each 10-cm by 10-cm cell by averaging all points inside the cell. The average number of points in any 10 cm x 10 cm cell was 3.89 (3,894 pts

m^{-2}). Natural Neighbor interpolation was specified as the void fill method (Sambridge et al., 1995). Point clouds, finalized DEMs, and representative photographs for each survey are available online, hosted by OpenTopography (Volpano et al., 2021a; Volpano et al., 2021b).

Two GCP's were taken during the surveys to estimate the error of the RTK SfM point cloud. The GCP's were surveyed using an Emlid Reach RS2 multi-band RTK GNSS receiver rover and base pair. The Reach RS2 positioning data were corrected against data from the Wisconsin Continuously Operating Reference Station (WISCORS) located 15 km from the site using RTKLIB PPK algorithms. The average vertical offset between the post-processed GCP's and P4RTK (SfM point cloud) locations for the surveys was ±0.05 m and ±0.04 m, respectively.

Nearshore Bathymetry

Nearshore bathymetry data was collected from a boat mounted echosounder to document nearshore geomorphic change and construct the XBeach model. Fixed-wing derived topobathy LiDAR surveys (1.5 m resolution) were available for the region (OCM Partners, 2021) but were conducted infrequently (~5-10 years apart) and did not capture the historic range of lake-level fluctuations. The time between LiDAR surveys was sufficiently long that nearshore change of the small-scale features (i.e., bars, beach slope) could change substantially, rendering the surveys of minimal use for high resolution morphodynamic modelling. Particularly in the context of lake level fluctuations, the LiDAR surveys did not cover the historic range, and the nearshore data might only be relevant for coastal modelling of a period of months or years. Additionally, these surveys only cover a portion of the coastline, resulting in data gaps for some sites. Predictive morphodynamic modelling of coastal evolution is time and scale dependent, and the reliance on antecedent morphology suggested it necessary to collect current nearshore bathymetric data for each survey period.

A Bathylogger BL200 200 kHz single beam echosounder (SBES) integrated with an Emlid Reach RS2 receiver was mounted to a 12 ft boat to collect bathymetric data. This setup was utilized to map 200 m alongshore from 0.5 m to 5 m depth, approximately 300 m offshore

(Figure 4) at a rate of 10 samples per second. Planned transects were cast perpendicular to the shore at 20 m spacing and uploaded to a LOWRANCE Hook2 7 Tripleshot fishfinder with GPS for navigation. The SBES returned a depth accuracy of ±1 cm for every 10 m depth (Bathylogger, 2018) and the survey depth did not exceed 5 m. Post-processed GPS error was ±0.009 m and ±0.006 m in the horizontal and vertical, respectively.

Cross-shore wading surveys were conducted using RTK GPS to cover the interface between subaqueous and subaerial surveys. Transects were spaced at approximately 20 m intervals alongshore. Cross-shore elevation was recorded at ~1 m spacing with finer spatial sampling at abrupt elevation changes and extended from the storm-highwater mark to approximately 1 m water depth. RTK-GPS data were post-processed using WISCORS reference stations and RTKLIB.

Following collection, the points from the various acquisition techniques were merged into a single topobathy dataset. Wading and bathymetry surveys were edited for spurious datapoints using a standard deviation threshold (Yin et al., 2013) in MATLAB. Drone survey data were sampled on 20 m spacing alongshore at a cross shore interval of 2 m. Bathymetry data were combined with beach and wading transects to generate a continuous profile of beach and nearshore. The data were interpolated to a rectilinear grid using the Kriging function in Surfer® from Golden Software, LLC (www.goldensoftware.com). The mean squared error between the measured soundings and points on the interpolated surface was ±0.0021 m for the first survey and ±0.0018 m for the second survey.

Wave Climate

Nearshore wave data are necessary to drive simulations of coastal processes. However, in situ nearshore data is sparse in the Great Lakes, necessitating the use of regional models for location specific data. Wave models from the National Oceanic and Atmospheric Administration (NOAA) Great Lakes Environmental Research Laboratory (GLERL) based on bathymetry datasets with three arc-second (about 90 m) resolution (Jensen et al., 2012) are available for the NAGL. Due to the coarse grid resolution of the basin-scale model, natural shoreline variability is not captured, leaving significant spatial gaps between the most shoreward grid cell and nearshore sites. Lake-wide models (NOAA-GLERL, 2020) are driven by meteorological data recorded at offshore buoys (NDBC, 2021).

Hourly modelled wave conditions were obtained from the Great Lakes Coastal Forecasting System (GLCFS; NOAA-GLERL, 2020) at the computational grid cell located nearest to the study area (~1 km offshore). Wave data from the GLCFS model (significant wave height, wave direction, and wave period) were used to drive the XBeach simulation at its lakeward boundary, approximately 300 m offshore. XBeach was used to model changes to waves as they approach the shoreline and began to shoal. To validate the XBeach estimates of GLCFS offshore wave transformation to the nearshore we deployed two RBR*solo*^{3} single-channel loggers at approximately 1.5 m depth (30 m from shore). The sensors recorded burst data at 10-minute intervals. One sensor was recovered, the other could not be recovered due to burial by an onshore migrating nearshore bar. Wave data from the recovered sensor was used to compare the in-situ wave conditions to modeled wave output from XBeach. The Root Mean Squared Error (RMSE) of significant wave height between datasets (GLCFS vs. RBR*solo*^{3}, RBR*solo*^{3} vs. XBeach) was computed. Data were resampled to the same hourly interval. RMSE was calculated for GLCFS and XBeach model outputs relative to the RBR*solo*^{3} sensor data collected in the nearshore.

Hydrodynamic Model Description

To model nearshore sediment transport at our study site we implemented XBeach-- an open-source numerical modelling program primarily developed for the simulation of coastal response to hurricanes, storm surge, dune evolution, and nearshore sediment transport (Roelvink et al., 2009). XBeach has three hydrodynamic regimes: Stationary, Nonhydrostatic, and Surfbeat. The Stationary mode solves wave averaged equations but does not resolve long (infragravity) or short (wind-generated) waves (Deltares, 2020). This formulation is most appropriate for long-term modelling due to its computational efficiency; however, the wave characteristics are less defined and therefore inaccurate for shorter term predictions. The Nonhydrostatic regime fully resolves the phase of individual long and short waves. Higher grid resolution is necessary for a Nonhydrostatic simulation, making it the most computationally intensive hydrodynamic option, and the sediment transport equations are not extensively validated. Surfbeat mode fully resolves long waves but averages short waves on the time scale of wave groups, applying a mean short-wave envelope (Deltares, 2020). Energy is propagated according to the short-wave action balance, and this mode is less computationally expensive because short waves are not phase resolved. Both the Nonhydrostatic and Surfbeat mode were applicable for the Great Lakes test case, however the Nonhydrostatic mode was less desirable because it is computationally intensive and sediment transport equations are not well validated. This study applied Xbeach (version 1.23.5526) in Surfbeat mode (hereafter XB-SB) to resolve nearshore dynamics. It should be noted that, because of the low-moderate wave conditions captured, a phase-resolving model would be most appropriate for the short-wave dominated climate. Our focus was on sediment transport for management purposes where computational efficiency is important, therefore we implemented XB-SB.

Using Xbeach we conducted sensitivity tests of the asymmetry and skewness parameter (see Electronic Supplementary Material (ESM) Appendix S1) to investigate the impact on nearshore sediment transport and assess model-data convergence. These parameters influence wave shape and have the most impact on model hydrodynamics for swash and dune erosion resulting from cross-shore flow velocities (Bugajny et al., 2013; Elsayed, 2017; Ruessink et al., 2007; 2011; Van de Ven, 2018; Zimmerman et al., 2015). Because XB-SB is not phase resolving, the asymmetry and skewness factor (*facua;* γ_{ua}), is integrated into the equations for sediment advection velocity (Elsayed, 2017). Increasing *facua* values increases the onshore sediment transport by waves. Simulations were run for *facua* between 0.0 and 0.60 at increments of 0.1, while other parameters were held constant.

XBeach Simulation

Topobathy, offshore wave data, and asymmetry/skewness values were integrated into boundary conditions for our XB-SB model. Default values for all other parameters were used unless noted below because they perform well for most wave scenarios (Deltares, 2020;

Trouw et al., 2012). Model grids were created using RGFGrid/QuickIn (Deltares, 2014) and MATLAB functions from the OpenEarth toolbox for XBeach (Deltares, 2016). The resulting grid dimensions were *nx* = 122 and *ny* = 46 and were of variable size ranging from 1 m to 12 m in the cross-shore and 2.5 m to 12 m alongshore (Figure 5). The wave spectrum discretization had a directional resolution of 20° and encompassed all directions towards the coast. We obtained wave data (height, period, and direction) for the ~600 simulated hours from the GLCFS. Grain size analysis was run on beach samples from the site using a Mastersizer 2000 laser diffraction instrument (e.g., Dias, 2014), and used to set the d_{50} and d_{90} grain size at 0.0003 m, 0.00044 m, respectively.

To reduce bias of error calculations resulting from the variable spacing of the XBeach morphologic grid the model predictions of final bed level were interpolated to a regularly spaced 1 m x 1 m grid using the Natural Neighbor technique (Sambridge et al., 1995). Performance of the model relative to baseline observations and final survey measurements was assessed using a metric known as the Brier Skill Score (Sutherland et al., 2004), but is more appropriately named the Mean Square Error Skill Score (MSESS; Bosboom, 2019). The MSESS decomposed the misfit between measured and modelled bathymetry into phase, amplitude, and a bias term (Murphy and Epstein, 1989; Sutherland et al., 2004; see ESM Appendix S2). Analysis of skill excluded the area inland of the dune crest due to grass and low vegetation that was not removed by filters and thus creates noise in the elevation data.

Results

Hydrodynamic Outputs

The RMSE of RBR*solo*^{3} and the GLCFS data was 0.299 m. The RMSE of the RBR*solo*^{3} and XBeach hydrodynamic output was 0.185 m. XBeach hydrodynamic outputs agree with measurements recorded by the pressure transducer for some waves, while it underpredicts others (Figure 6). Attenuated measurement data is observed around September 5 when upon retrieval the sensor was buried under several inches of sand. We hypothesize that a period of energetic waves buried the sensor around September 4. Waves are also overpredicted by XBeach around September 2, which we attribute to similar circumstances of sensor burial.

Underprediction of wave height by XBeach seems primarily related to the angle of incidence of the waves input at the offshore boundary. Offshore waves occurring between 150° and 300° generate no nearshore waves in XBeach because they travel away from shore and out of the model domain. These offshore directed waves are likely driven by wind energy, which is not implemented in XB-SB. The largest waves observed during the study period originated north of the site, but the majority of waves approached from the east-southeast.

Measured Change

Visual analysis of cross shore profiles shows the bar nearest to shore was translated onshore between surveys, infilling the most shoreward trough (Figure 7). The DEM of difference (DoD) displays net erosion, where the inner and middle bars were planed off, and net accretion shoreward, where there was infilling of the troughs. This infilling suggests that the nearshore bar is welding to the beach face, as observed in previous studies of low wave energy conditions in the NAGL (Davis and Fox, 1972; Hands, 1984; Houser and Greenwood, 2005). Erosion at the interface between subaerial/subaqueous beach was most apparent on the northern half of the shoreline. Minimal change was observed near the offshore survey boundary.

Asymmetry & Skewness Model Runs

The results of the lowest (0.1) and highest (0.6) *facua* runs are shown in Figure 8. Figure 8A and 8B are DoDs between the final bathymetry output by the model and the initial model bathymetry. The lower *facua* runs depict greater magnitude shoreline erosion, particularly in the southern region. Higher *facua* runs predict less sediment transport overall and increased deposition in the center of the model domain.

Final bathymetry outputs for the *facua* calibration show the most change in the swash zone in the southern part of the model domain. The default value (*facua* = 0.1) produces substantial scouring of the trough nearest to shore that is inconsistent with observed changes. Higher values of *facua* predict an accumulation of sediment in the same trough, which is more similar to the surveyed changes. Figure 8C shows a cross sectional profile in the center of the model domain of predicted final bed morphology for the lowest (0.1) and highest (0.6) *facua* runs. All model runs overpredict erosion near the offshore limit of the model domain, on the scale of decimeters. The three nearshore bars translate offshore in all model runs, opposed to the onshore translation that was actually measured in surveys. The models generally did not predict the scouring of the middle bar or the infilling of the trough nearest to shore (bar welding). Model runs had more variability across the domain close to shore. The outer bar was predicted to move offshore, contrasting with survey results, but this prediction was consistent across a range of *facua* values. The middle and inner bars, however, demonstrated greater variability in response to changing asymmetry and skewness.

Skill Score

The MSESS and decomposition (*3.1.3 Wave Climate*; ESM Appendix S2) values for the different model runs are given in Table 1. The phase error, amplitude error, and map mean error improve slightly as *facua* is increased. The same holds for the final computed MSESS, although negative values suggest that the final modelled bathymetry diverges from the final measured bathymetry more than the initial model bathymetry. Decomposition of the MSESS can elaborate on how distinct aspects of the model performed. Low values for the phase alignment (α) suggest that sand is either moved to the wrong location within the model, or that the shape and amplitude of nearshore features is incorrect (Bosboom, 2019; Sutherland et al., 2004). In this case, offshore bar movement was predicted by the model, but measurements showed a shoreward translation. Amplitude error (β) scores are good overall, suggesting that the amount of sand fluxed within the model domain is consistent to the observed sediment transport, especially for higher values of *facua.* The map mean error (γ) is a measure of the difference between the predicted average bed level and the measured average bed level. The map mean error is low overall and becomes closer to the ideal value as *facua* increases. This is likely a function of morphology changes that are localized to a small percentage of the total map area.

Discussion

A well-developed berm formed along the upper shoreface of the site between the August and September surveys (Figure 7B). This is consistent with conceptual models of shoreface evolution under low wave-energy conditions where sediment is commonly transported shoreward and welds to the beach (Masselink et al., 2006; Plant et al., 1999). Erosion did not occur along the foredune or backshore, and profile changes landward of the foredune crest are attributed to changes in low vegetation not recognized during filtering. The lack of dune erosion is consistent with the low wave-energy conditions observed during the study (most waves less than 0.5 m), which were unable to reach the upper shoreface even during seasonal high lake levels. Bathymetric changes were negligible in depths greater than 3 m (Figure 7B). Erosion becomes more pronounced moving towards the shore, where the outer bar (x = 160 m) is eroded, and the associated shoreward trough is slightly infilled. The inner bar (x = 75 m) widened in the cross-shore direction and the crest migrated landward approximately 10 m. Sediment also accreted in the most shoreward trough, which we attribute to the process of the bar welding to the shoreline. This pattern of shore-parallel alternating erosion and deposition is characteristic of landward bar migration (Hands, 1984). Following periods of storm activity, low energy conditions can cause bars to migrate landward and weld to the beach as part of the recovery process. The morphological changes observed suggest that continued low wave-energy conditions could lead to the inner bar welding to the foreshore at our site.

The skill score calculations for all model runs during this period of low wave amplitudes are generally poor (Table 1), however skill scores can be difficult to interpret for only small changes (Sutherland et al., 2004; ESM Appendix S2). Model skill scores of <0 for all runs, signify that the difference between the model output and the final bathymetry survey was larger than from the initial baseline elevation survey. Therefore, we can only develop a relative scale of skill for our modelling efforts, while acknowledging that none of our runs truly represented the conditions well. The slope of the shoreface in this model domain is consistent with the use of a higher value of *facua* due to increased nonlinearity for shallow slopes (Brinkemper, 2013). The MSESS improves (becomes less negative) for higher values of *facua,* but potential limitations of the skill score should be considered. First, although horizontal and vertical error was low for our RTK-GPS dataset, transects were spaced ~20 m apart, thus elevation data was interpolated between these transects. The MSESS score does not account for the discrepancies between the real bed elevation and interpolated bed elevations in areas between transects. Any error in the interpolation causes the MSESS to penalize the hydrodynamic model, which factors into the efficacy of skill estimation (Sutherland et al., 2004). Most importantly, the scores may be poor because measured differences in bathymetry during the survey period were small, owing to the relatively low wave conditions throughout the study period. In such cases, even small dissimilarities between the modelled and measured final bathymetries can significantly factor into the skill score (see ESM Appendix S2). A tendency of MSE based metrics is to reward underprediction of morphologic change and penalize variability in the morphology if it is not accurate (Sutherland et al. 2004). An exceedingly high model accuracy is required to surpass the skill score from a simulation that (incorrectly) predicts zero change. This becomes difficult when the magnitude of change is small (as in our case). Therefore, when slight changes are observed the MSESS is not ideal for calculating the overall skill of the model (Sutherland et al., 2004). The MSESS results can, however, be used to rank relative skill of model runs but does not necessarily give a reliable metric of performance. The decomposition into phase, amplitude, and map mean error provide an assessment of different components of the model. Particularly, the amplitude error scores suggest that the amount of sediment moved within the model domain is consistent with what was measured (Table 1).

Although it is established that large waves coupled with high lake levels cause significant erosion (e.g., Baird, 2010; Brown et al., 2005; Dubois 1973; Theuerkauf et al., 2021), our ~1 month study period was dominated by low-moderate waves that generally promote beach recovery. The timescale of bar response to lake level change and storm conditions is of interest for further study into beach recovery. When coasts are exposed to long-period swells for extended periods of time (~weeks) bars can migrate onshore during the subsequent period of non-storm activity (Davis and Fox, 1972). During our ~1 month study we observed an average wave period of 3 sec (NOAA-GLERL 2020), consistent with a slow rate of onshore bar migration due to the absence of long period swells. Our modelling results showed that XBeach was not capable of simulating the process of onshore bar migration and welding associated with beach recovery in the NAGL. These processes must be resolved in order to successfully predict antecedent morphology establishes the vulnerability of a coastal site to storms (Theuerkauf et al., 2021). The formulation of the governing equations of XBeach Surfbeat suggests depiction of erosion and sediment transport is better resolved for larger wave energy. However, it would appear from our results that XBeach is not well suited to simulate the recovery between storm events.

Additionally, nearshore hydrodynamic processes excluded from the parameter sweep could potentially be important for realistic modelling of low-moderate wave conditions in the NAGL. Although the skewness/asymmetry parameter is cited as the most significant influence on final bathymetry (Bugajny et al., 2013; Elsayed, 2017; Ruessink et al., 2007; 2011; Van de Ven, 2018; Zimmerman et al., 2015), it is possible the model may have better simulated low wave conditions if additional parameters were assessed. For example, significant physical parameters such as critical avalanching slope, equilibrium sediment concentration formulation, short wave turbulence, and wave group energy propagation (Roelvink et al., 2018; Vousdoukas et al., 2012) may have affected the results. However, these parameters increase in importance as the beach slope increases, and so for the low-angle dissipative beach examined in this study these likely would provide only modest improvements. Longshore currents, growth by wind forcing, and lake-wide water level fluctuations were also not included, but longshore currents are typically low in Lake Michigan during the summer months (Mao and Xia, 2021). Li (2021) found through sediment transport modelling near a Lake Michigan harbor that longshore transport is an order of magnitude greater than cross-shore during low wave conditions, but due to alternating current directions there is little net transport in the alongshore direction. Additionally, Li (2021) notes that wind generated surface currents offshore have little capacity to influence nearshore sediment transport during low wave periods. Therefore, it is unlikely that adding surface current data (*e.g.* from the GLCFS) at the model boundaries would significantly impact our findings related to sediment transport. Lake level fluctuations were also not included in this modelling effort but were minimal over the 1-month period. Significant fluctuations of lake level occur on a seasonal time scale, the range of values observed during our study was -0.204 m to 0.085 m from the water level at the time of the initial survey, which is too low to be significant in the short term. In summation while numerous additional factors could have been incorporated to improve the modeling effort it is unlikely that any of them would exert a first order control on sediment transport and improve the model results significantly at our site over the time range of the study.

Hands (1984) found that several storm seasons are required to readjust NAGL nearshore profiles with a lake level increase of tenths of a meter, meaning nearshore wave conditions and bar morphology are in disequilibrium for substantial periods of time. Plant et al., (1999) demonstrated a lag time between wave conditions and bar evolution, where transient bar formation persists over interannual scales. These studies show that nearshore readjustment may take more than a single season in the NAGL. The elevation changes we observed in our cross-shore profile suggest an increase in accommodation space. The overall trend of lake levels during this period is decreasing (Figure 1A), but the lake level peak in 2020 was greater than the peak measured in 2019. This lag indicates that bar movement is not perfectly coupled to lake level. The observations of a lag between peak lake levels and peak shoreline erosion (Plant et al., 1999) and the persistence of high erosion after lake level decreases (Hands, 1984) suggest that the effects of fluctuating lake levels are relevant for several years after water level change. Although lake levels have dropped below the records set throughout the 2020 season, questions related to sediment transport and increased erosion will persist into the future.

Numerical modelling of nearshore hydrodynamics of the NAGL is necessary to study the complex interactions between morphology and varying water levels, sediment supply, and storms to guide coastal management actions. We find that XBeach Surfbeat is not capable of simulating small morphology changes in the NAGL associate with beach recovery accurately. It is possible that the phase resolving model, i.e., XBeach Nonhydrostatic, may better replicate the low wave energy morphodynamic evolution. However, the sediment transport equations are not extensively tested (Deltares, 2020) and it is computationally intensive and so its use for management decisions may be diminished. XBeach Surfbeat is well validated for sandy beach evolution under energetic wave conditions in oceans and estuaries (Harley et al. 2011; McCall et al. 2010; Roelvink et al. 2009; Van Thiel de Vries 2010; Vousdoukas et al. 2011a;), therefore, the model should be able to simulate coastal response to large storms in the Great Lakes and future studies should focus on testing this. To accurately simulate the full suite of geomorphic responses in the NAGL (i.e., storm response and beach recovery) XBeach may need to be coupled to a model that captures beach recovery well (i.e., Delft3D (e.g., van Dam 2019)) thereby improving the ability for a model to predict the actual physical vulnerability of a Great Lakes coastal site.

Conclusions

This work investigates the morphological evolution of a barred nearshore site during a period of quiescent wave activity in the NAGL to examine whether a widely used and efficient numerical model can simulate beach recovery processes in the NAGL. XBeach-Surfbeat was used to represent the 2DH wave propagation and sediment transport over the three-dimensional bar system. This study aims to add to the few morphological modelling studies performed in the NAGL that link environmental forcing to shoreline erosion and sediment movement in the nearshore. Our results show that hydrodynamic formulations in XBeach-Surfbeat and model configuration in our study are not effective at modelling coastal change during periods of high lake level and low wave energy (Figure 8). Favorable scores for the amplitude error show that the correct volume of sediment was moved within the model, while high error scores overall show the sediment was moved to the wrong place. Changes in measured bathymetry between surveys are consistent with morphologic evolution under high lake level and low wave energy conditions expected during beach recovery based on previous studies (Davidson-Arnott, 1988; Davis and Fox, 1972; Davis et al., 1972; Hands, 1984). During these times, the energy inputs are dominated by short wave energy and so the phase-averaging nature of the Surfbeat mode cannot accurately capture the processes in the NAGL. Coastal morphodynamic modelling can aid in understanding large scale changes in the NAGL nearshore caused by storms and lake level fluctuations, but we find XBeach Surfbeat is of limited value for small scale wave events that drive beach recovery in the NAGL.

Acknowledgments

Many thanks to the staff at Point Beach State Forest for access to the study area. This project was supported by UW Sea Grant awards R/RCE-16 and R/RCE-19, the Wisconsin Geological and Natural History Survey, the Woolard fund and LKZ, JER, EJT were partially supported by NSF Award Numbers:1916179 and 1950101

References

Aerotas, 2018. Phantom 4 RTK PPK Processing Workflow. [WWW Document]. URL https://www.aerotas.com/phantom-4-rtk-ppk-processing-workflow (accessed 6.4.21)

Angel, James R., and Scott A. Isard. 1998. The Frequency and Intensity of Great Lake Cyclones. *Journal of Climate* 11 (1): 61–71.

As-Salek, J.A., and Schwab, D., 2002. High-frequency water level fluctuations in Lake Michigan. Journal of Waterway, Port, Coastal, and Ocean Engineering. Vol. 130 (1).

Baird, W.F., Associates Ltd., 2010. Erosion Theme Report (No. 11526.200). International Joint Commission Coastal Zone Technical Working Group.

Baird, W.F., Associates, 2008. FEPS sensitivity analysis for the International Upper Great Lakes Study (No. 10970.000). International Upper Great Lakes Study.

Bamunawala, Janaka, Ali Dastgheib, Roshanka Ranasinghe, Ad van der Spek, Shreedhar Maskey, A. Brad Murray, Trang Minh Duong, Patrick L. Barnard, and T. A. J. G. Sirisena. 2020. A Holistic Modeling Approach to Project the Evolution of Inlet-Interrupted Coastlines Over the 21st Century. *Frontiers in Marine Science* 7: 542. https://doi.org/10.3389/fmars.2020.00542

Barnard, P.L., Erikson, L.H., Foxgrover, A.C., Hart, J.A.F., Limber, P., O'Neill, A.C., van Ormondt, M., Vitousek, S., Wood, N., Hayden, M.K., Jones, J.M., 2019. Dynamic flood modeling essential to assess the coastal impacts of climate change. Sci. Rep. 9, 4309.

Barnard, P.L., van Ormondt, M., Erikson, L.H., Eshleman, J., Hapke, C., Ruggiero, P., Adams, P.N., Foxgrover, A.C., 2014. Development of the Coastal Storm Modeling System (CoSMoS) for predicting the impact of storms on high-energy, active-margin coasts. Nat. Hazards 74, 1095–1125.

Bathylogger, 2018. BL200 Single Beam Echo Sounder. [WWW Document]. URL https://bathylogger.com/product/bl200-single-beam-echo-sounder/ (accessed 6.4.21)

Booth, J.S., 1994. Wave climate and nearshore lakebed response, Illinois Beach State Park, Lake Michigan. J. Great Lakes Res. 20, 163–178. https://doi.org/10.1016/S0380-1330(94)71138-2.

Bosboom, J., 2019. Quantifying the quality of coastal morphological predictions. TU Delft. https://doi.org/10.4233/uuid:e4dc2dfc-6c9c-4849-8aa9-befa3001e2a3

Braun, Katherine N., and Ethan J. Theuerkauf. 2021. "The Role of Short-Term and Long-Term Water Level and Wave Variability in Coastal Carbon Budgets." *iScience* 24 (5): 102382.

Brown, E.A., Wu, C.H., Mickelson, D.M., Edil, T.B., 2005. Factors controlling rates of bluff recession at two sites on Lake Michigan. J. Great Lakes Res. 31, 306-321.

Bugajny, N., Furmańczyk, K., Dudzińska-Nowak, J. & Paplińska-Swerpel, B., 2013. Modelling morphological changes of beach and dune induced by storm on the Southern Baltic coast using XBeach (case study: Dziwnow Spit). Journal of Coastal Research SI, 65, 672-677.

Cavaleri, L., Abdalla, S., Benetazzo, A., Bertotti, L., Bidlot, J.R., Breivik, Ø., Carniel, S., Jensen, R.E., Portilla-Yandun, J., Rogers, W.E., Roland, A., Sanchez-Arcilla, A., Smith, J.M., Staneva, J., Toledo, Y., van Vledder, G.Ph., van der Westhuysen, A.J., 2018. Wave modelling in coastal and inner seas. Progress in Oceanography, Volume 167, 164-233, ISSN 0079-6611, https://doi.org/10.1016/j.pocean.2018.03.010.

Chrzastowski, M.J., Thompson, T.A., Brian, Trask C., 1994. Coastal geomorphology and littoral cell divisions along the Illinois-Indiana coast of Lake Michigan. J. Great Lakes Res. 20 (1), 27–43

Davidson-Arnott R.G.D., 2010. Introduction to coastal processes and geomorphology. United States of America by Cam-bridge University Press, New York.

Davidson-Arnott, R.G.D., 1988. Controls on formation and form of barred nearshore profiles. Geographical Review. 185-193. DOI: 10.2307/214176

Davidson-Arnott, R.G.D., 1989. The effect of water level fluctuations on coastal erosion in the Great Lakes. Ontario Geography. 33, 23-39.

Davidson-Arnott, R.G.D., and van Heyningen, A.G., 2003. Migration and sedimentology of longshore sandwaves, Long Point, Lake Erie, Canada. Sedimentology. 50, 1123-1137.

Davis, R.A., and Fox, W.T., 1972. Coastal processes and nearshore sand bars. SEPM J. Sediment. Res. 42, 401–412. https://doi.org/10.1306/74D72568-2B21-11D7-8648000102C1865D.

Davis, R.A., Jr., and Fox, W.T., 1976. Simultaneous process-response study on the east and west coasts of Lake Michigan, J. Great Lakes Res., 2, 27-32.

Deltares, 2014. “QuickIn” & “RGFGrid” (version 4.00.34158). obtained from https://oss.deltares.nl/web/delft3d/source-code

Deltares, 2016. “OpenEarth Matlab Toolbox for XBeach” (revision 5481). Obtained from https://publicwiki.deltares.nl/display/OET/OpenEarth+Product+Suite

Deltares, 2020. “XBeach User Manual” (Revision 51bb68d9). https://xbeach.readthedocs.io/en/latest/user_manual.html

Dias, K.A., 2014. High-resolution methodology for particle size analysis of naturally occurring sand size sediment through laser diffractometry with application to sediment cores: Kisment, Fire Island, New York. M.S. Thesis, Stony Brook University.

Dibajnia, M., Nair, R.B., Ross, P., 2004. Analysis of long-term sand accumulation at a harbor using 2DH numerical simulation. Coastal Engineering. 51, 863-882.

Dott, E.R., and Mickelson, D., 1995. Lake Michigan water levels and the development of Holocene beach-ridge complexes at Two Rivers, Wisconsin: Stratigraphic, geomorphic, and radiocarbon evidence. GSA Bulletin 107(3) 286-296. https://doi.org/10.1130/0016-7606(1995)107<0286:LMWLAT>2.3.CO;2

DuBois, R.N., 1973. Seasonal variation of a limnic beach. Geological Society of America Bulletin. 84, 1817-1824.

Elsayed, S.M., Oumeraci, H., 2017. Breaching of Coastal Barriers under Extreme Storm Surges and Implications for Groundwater Contamination: Improvement and Extension of the XBeach Model to Account for New Physical Processes (PhD). Leichtweiß-Institute for Hydraulic Engineering and Water Resources.

Emery, K.O., 1961. A simple method of measuring beach profiles. Limnology and Oceanography. 6(1) 90-93.

Fox, W.T., Davis Jr., R.A., 1973b. Simulation model for storm cycles and beach erosion on Lake Michigan: Geol. Soc. Amer. Bull.,v. 84, p. 1769-1790.

Fry, L.M., Apps, D., Gronewold, A.D., 2020. Operational seasonal water supply and water level forecasting for the Laurention Great Lakes. Journal of water resources planning and management, 2020-09-01, Vol. 146 (9). P. 4020072. https://doi.org/10.1061/(ASCE)WR.1943-5452.0001214.

Gallagher, G.E., Duncombe, R.K., Steeves, T.M., 2020. Establishing Climate Change Resilience in the Great Lakes in Response to Flooding. Journal of Science Policy & Governance, 17-1.

Great Lakes Coastal Resilience Planning Guide, 2018. Great Lakes Coastal Resilience Planning Guide. National Oceanic and Atmospheric Association. https://greatlakesresilience.org/

Gronewold, A. D., Do, H. X., Mei, Y., & Stow, C. A. (2021). A tug-of-war within the hydrologic cycle of a continental freshwater basin. *Geophysical Research Letters*, 48, e2020GL090374. https://doi.org/10.1029/2020GL090374

Hands, E.B., 1979. Changes in Rates of Shore Retreat, Lake Michigan, 1967-76. USACE Coastal Engineering Research Center, Technical Paper No. 79-4.

Hands, E.B., 1984. The Great Lakes as a Test Model for Profile Response to Sea Level Changes. US Army Corps of Engineers Miscellaneous Paper CERC-84-14. Coastal Engineering Research Center.

Harley, M., Armaroli, C., Ciavola, P., 2011. Evaluation of XBeach predictions for a real-time warning system in Emilia-Romagna, Northern Italy. J Coast Res SI 64:1861-1865.

Houser, C. and Greenwood, B, 2007. Onshore migration of a swash bar during a storm. Journal of Coastal Research, 231:1-14.

Houser, C. and Greenwood, B., 2005. Profile response of a lacustrine multiple barred nearshore to a sequence of storm events. Geomorphology, 69: 118-137.

Isenburg, M., 2014. "LAStools - efficient LiDAR processing software" (version 141017, unlicensed), obtained from http://rapidlasso.com/LAStools

Jensen, R.E., Cialone, M.A., Chapman, R.S., Ebersole, B.A., Anderson, M., and Thomas, L., 2012. Lake Michigan storm: Wave and water level modelling. U.S. Army Engineer Research and Deveopment Center, EDRC TR-12-X.

Krueger, R., Zoet, L. K., & Rawling, J. E. III, 2020. Coastal bluff evolution in response to a rapid rise in surface water level. Journal of Geophysical Research: Earth Surface, 125, e2019JF005428. https://doi.org/10.1029/2019JF005428

Lake Huron Centre for Coastal Conservation, 2019. Coastal Action Plan for the Southeastern Shoreline of Lake Huron. Goderich, Ontario.

Li, H., 2021. Transport of placed dredged material in surf and nearshore zone. J. Waterway, Port, Coastal, Ocean Eng. 147(3): 05021002 1-18.

Mao, M., & Xia, M., 2020. Monthly and Episodic Dynamics of Summer Circulation in Lake Michigan. Journal of Geophysical Research: Oceans, 124, e2019JC015932. https://doi.org/ 10.1029/2019JC01593

Masselink, G., Puleo, J.A., 2006. Swash-zone morphodynamics. Continental Shelf Research, Vol. 26 (5) .pp. 661-680. https://doi.org/10.1016/j.csr/2006.01.015.

Mattheus, C.R., 2016. GIS-based geomorphologic study of Presque Isle Peninsula, a compound lacustrine barrier-spit system along the south-central Lake Erie margin. Journal of Great Lakes Research Vol. 41, 2. Pp. 336-347.

Mattheus, C.R., Climate-Induced Changes in Rates of Headland-Beach Progradation along the Southern Coast of Lake Erie. *Journal of Coastal Research* 1 July 2014; 30 (4): 743–755. doi: https://doi.org/10.2112/JCOASTRES-D-13-00156.1

Mattheus, C.R., Diggins, T.P., Boyce, C., Cockrell, J., Kruske, M., VanWinkle, M., 2019. Geomorphology of a harbor-breakwater beach along a high sand-supply, wave-dominated Great Lakes littoral cell. J. Coastal Res. 35(1), 41-55. https://doi.org/10.2112/JCOASTRES-D-17-00209-1.

Mattheus, C.R., Fowler, J.K., Diggins, T.P., 2017. Hydrodynamic and sediment-accomodation controls on headland-beach geomorphology evaluated by statistical methods, southern Lake Erie coast. Journal of Great Lakes Research, Vol 43 (2). Pp 228-238.

McCall, R.T., Van Thiel de Vries, J.S.M., Plant, N.G., Van Dongeren, A.R., Roelvink, J.A., Thomson, D.M., Reniers, A.J.H.M., 2010. Two-dimensional time dependent hurricane overwash and erosion modeling at Santa Rosa Island. Coastal Eng 57(7):668-683. Doi: 10.1016/j.coastaleng.2010.02.006.

Meadows, G. A., L. A. Meadows, W. L. Wood, J. M. Hubertz, M. Perlin, G. A. Meadows, L. A. Meadows, W. L. Wood, J. M. Hubertz, and M. Perlin. 1997. "The Relationship between Great Lakes Water Levels, Wave Energies, and Shoreline Damage." *Bulletin of the American Meteorological Society* 78 (4): 675–82.

Metashape, 2020. Agisoft Metashape User Manual: Professional Edition, Version 1.6. Agisoft LLC.

Mickelson, D.M., and Socha, B.J., 2017. Quaternary Geology of Calumet and Manitowoc Counties, Wisconsin. UW Extension Bulletin 108.

Morang, A., Dunkin, L.M., Bucaro, D.F., Wethington, J.A., Chrzastowski, M.J., Theuerkauf, E.J., 2019. Sediment budget for North Illinois shore from the Wisconsin border to Wilmette

Harbor. US Army Corps of Engineers, Coastal and Hydraulics Labratory ERDC/CHL TR-19-13.

Morang, A., Mohr, M.C., Forgette, C.M., 2011. Longshore sediment movement and supply along the U.S. shoreline of Lake Erie. J. Coastal Res. 27(4), 619-635.

Murphy, A.H., Epstein, E.S., 1989. Skill scores and correlation coefficients in model verification. Monthly Weather Review 117, 572-581.

Nairn, R.B., and Southgate, H.N., 1993. Deterministic profile modelling of nearshore processes- Part 2: Sediment transport and beach profile development. Coastal Engineering 19, 57-96.

Nairn, R.B., Zuzek, P.J., 2005. Automated lake wide erosion predictions and economic damages on Lake Ontario. ASCE. Solutions to Coatal Disasters 2005.

National Data Buoy Center (NDBC), 2021. Station 45007 (South Michigan). National Oceanic and Atmospheric Administration (NOAA). June 1, 2021.

National Oceanic and Atmospheric Administration (NOAA) -Great Lakes Environmental Research Laboratory (GLERL), 2020. Great Lakes Coastal Forecasting System, GLCFS. https://www.glerl.noaa.gov/res/glcfs/form.html

OCM Partners, 2021. 2012 USACE Great Lakes Topobathy Lidar: Lake Michigan (Wisconsin and Michigan) from 2010-06-15 to 2010-08-15. NOAA National Centers for Environmental Information, https://www.fisheries.noaa.gov/inport/item/49735.

Plant, N.G., R.A. Holman, M.H. Freilich, and W. A. Birkemeier, 1999. A simple model for interannual sandbar behavior. J. Geophys. Res., 104, 15,755–15,776, 1999.

Quinn, Frank H. 2002. "Secular Changes in Great Lakes Water Level Seasonal Cycles." *Journal of Great Lakes Research* 28 (3): 451–65.

Ranasinghe, R., 2016. Assessing climate change impacts on open sandy coasts: A review. Earth Science Reviews, 160, 320-332. Doi: 10.1016/j.earscirev.2016.07.011.

Reif, M., Wozencraft, J.M., Dunkin, L.M., Sylvester, C.S., Macon, C.,L., 2013. A review of U.S. Army Corps of Engineers airborne coastal mapping in the Great Lakes. Journal of Great Lakes Research, Vol. 39(1), p. 194-204. https://doi.org/10.1016/j.jglr.2012.11.002

Roelvink D., Boutmy A., and Stam, J.M., 1999. A Simple Method to Predict Long-Term Morphological Changes. *Coastal Engineering*, 3224–37.

Roelvink, D., McCall, R., Mehvar, S., Nederhoff, K., Dastgheib, A., 2018. Improving predictions of swash dynamics in XBeach: The role of groupiness and incident-band runup. Coastal Engineering 134, 103-123.https://doi.org/10.1016/j.coastaleng.2017.07.004

Roelvink, D., Reniers, A., van Dongeren, A., van Thiel de Vires, J., McCall, R., and Lescinski, J., 2009. Modelling storm impacts on beaches, dunes, and barrier islands. Coastal Engineering 56 (2009) 1133-1152. Doi:10.1016/j.coastaleng.2009.08.006.

Roland, C.J., L.K. Zoet, J.E. Rawling, M. Cardiff,2021. Seasonality in cold coast bluff erosion processes, Geomorphology, Volume 374, 107520, ISSN 0169-555X, https://doi.org/10.1016/j.geomorph.2020.107520.

Ruessink, B. G., Kuriyama, Y., Reniers, A. J. H. M., Roelvink, J. A., and Walstra, D. J. R. (2007), Modeling cross-shore sandbar behavior on the timescale of weeks, *J. Geophys. Res.*, 112, F03010, doi:10.1029/2006JF000730. asymmetric waves above a plane bed. Journal of Geophysical Research, 114, C11021.

Ruessink, B.G. , Michallet, H., Abreu, T. , Sancho, F. , van der A, D.A. , van der Werf, J.J., & Silva, P.A., 2011. Observations of velocities, sand concentrations, and fluxes under velocity-asymmetric oscillatory flows. Journal of Geophysical Research, 116, C03004 10.1029/2010JC006443

Sambridge, Malcolm, Jean Braun, and Herbert McQueen. 1995. "Geophysical Parametrization and Interpolation of Irregular Data Using Natural Neighbours." *Geophysical Journal International* 122 (3): 837–57.

Sellinger, Cynthia E., Craig A. Stow, E. Conrad Lamon, and Song S. Qian. 2008. "Recent Water Level Declines in the Lake Michigan-Huron System." *Environmental Science & Technology* 42 (2): 367–73.

Shabica, C.W., Mohr, M.C., Nagelback, S., 2011. Effects of structurally engineered beaches on coastal processes and shores of the Great Lakes. Shore & Beach. 78(4)/79(1), 51-63.

Sherwood, C. R., C. K. Harris, W. R. Geyer, and B. Butman (2002) Toward a Community Coastal Sediment-Transport Modeling System: Report of the Second Workshop, Eos, Transactions, American Geophysical Union, 83(51).

Sherwood, C. R., R. P. Signell, C. K. Harris, and B. Butman (2000) Workshop Discusses Community Models for Coastal Sediment Transport, Eos, Transactions, American Geophysical Union, 81(43): 502.

Sutherland, James & Peet, A. & Soulsby, R., 2004. Evaluating the performance of morphological models. Coastal Engineering 51, 917-939. Doi: 10.1016/j.coastaleng.2004.07.015.

Swenson, M.J., Wu, C.H., Edil, T.B., Mickelson, D.M., 2006. Bluff recession rates and wave impacts along the Wisconsin Coast of Lake Superior. J. Great Lakes Res. 32 (3), 512-530.

Takasu, T., 2018. "RTKLIB: An Open Source Program Package for GNSS Positioning" (version 2.4.3 p13). Obtained from http://www.rtklib.com/

Theuerkauf, Ethan J., and Antonio B. Rodriguez. 2012. "Impacts of Transect Location and Variations in Along-Beach Morphology on Measuring Volume Change." *Journal of Coastal Research* 28 (3): 707–18.

Theuerkauf, Ethan, C. Robin Mattheus, Katherine Braun, and Jenny Bueno. 2021. "Patterns and Processes of Beach and Foredune Geomorphic Change along a Great Lakes Shoreline: Insights from a Year-Long Drone Mapping Study along Lake Michigan." *Shore & Beach*. https://doi.org/10.34237/1008926.

Thompson, Todd A., and Steve J. Baedke. 1995. "Beach-Ridge Development in Lake Michigan: Shoreline Behavior in Response to Quasi-Periodic Lake-Level Events." *Marine Geology* 129 (1-2): 163–74.

Trouw, K., Zimmerman, N., Matys, M., Delgado, R., Roelvink, D., 2012. Numerical modelling of hydrodynamics and sediment transport in the surf zone: A sensitivity study with different types of numerical models. Coastal Engineering 2012.

Van Dam, T., 2019. Numerical modelling of beach recovery following a storm event. PhD Thesis. Delft University of Technology, Delft. http://repository.tudelft.nl/

Van de Ven, M.J.P., 2018. The effects of currents on wave nonlinearities. PhD Thesis. Delft University of Technology, Delft. http://repository.tudelft.nl/.

Van Thiel de Vries, J.S.M., 2010. Dune erosion during storm surges. PhD Thesis. Delft University of Technology, Delft.

Volpano, C., 2021a. Survey of Point Beach, Wisconsin, September 2020. Distributed by OpenTopography. https://doi.org/10.5069/G91V5C5J. Accessed: 2021-07-08.

Volpano, C., 2021b. Survey of Point Beach, Wisconsin, August 2020. Distributed by OpenTopography. https://doi.org/10.5069/G9X63K4B. Accessed: 2021-07-08.73.

Volpano, C.A., Zoet, L.K., Rawling, J.E. III, Theuerkauf, E.J., and Krueger, R., 2020. Three-dimensional bluff evolution in response to seasonal fluctuations in Great Lakes water levels. Journal of Great Lakes Research 46, 1533-1543.

Vousdoukas, M.I., Almeida, L.P, Ferreira, Ó.., 2011a. Modelling storm-induced beach morphological change in a meso-tidal, reflective beach using XBeach. J Coast Res SI64: 1916-1920.

Vousdoukas, M.I., Ferreira, Ó., Almeida, L.P., Pacheco, A., 2012. Toward reliable storm-hazard forecasts: XBeach calibration and its potential application in an operational early-warning system. Ocean Dynamics 62, 1001–1015 (2012). https://doi.org/10.1007/s10236-012-0544-6

Warner, John C., Christopher R. Sherwood, Richard P. Signell, Courtney K. Harris, and Hernan G. Arango. 2008. "Development of a Three-Dimensional, Regional, Coupled Wave, Current, and Sediment-Transport Model." *Computers & Geosciences* 34 (10): 1284–1306.

Westoby, J. Brasington, N.F. Glasser, M.J. Hambrey, J.M. Reynolds, 2012. 'Structure-from-Motion' photogrammetry: A low-cost, effective tool for geoscience applications. Geomorphology 179, 300-314. https://doi.org/10.1016/j.geomorph.2012.08.021

Wright, L.D., and Short, A.D., 1984. Morphodynamic variability of surf zones and beaches: A Synthesis. Mar. Geol., 56: 93-118.

Yin, Y., Wan., W. and Liu, R., 2013. Filtering outliers using statistical analysis on neighbors' distances. IET International Conference on Smart and Sustainable City 2013, 2013, pp 149-152. Doi: 10.1048/cp.2013.1993.

Zimmermann, N.; Trouw, K.; De Maerschalck, B.; Toro, F.; Delgado, R.; Verwaest, T.; Mostaert, F., 2015. Scientific support regarding hydrodynamics and sand transport in the coastal zone:

Evaluation of XBeach for long term cross-shore modelling. Version 3.0. WL Rapporten, 00_072. Flanders Hydraulics Research & IMDC: Antwerp, Belgium

Table 1: Mean squared error skill score and decomposition proposed by Murphy and Epstein (1989; see ESMAppendix S2).

facua	α	β	γ	MSESS
0	0.003	0.195	0.012	-0.205
0.1	0.002	0.132	0.003	-0.133
0.2	0.000	0.127	0.001	-0.129
0.3	0.000	0.072	0.001	-0.072
0.4	0.003	0.047	0.001	-0.044
0.5	0.007	0.034	0.000	-0.027
0.6	0.012	0.024	0.000	-0.012
Perfect Modelling	1	0	0	1

Figure 1: Selected hydrodynamic conditions for Lake Michigan, 2020. Dates of the study period highlighted in grey. A) Daily mean water level obtained from Kewaunee, WI. NOAA Station ID 9087068. B) Hourly output of significant wave height from the Great Lakes Coastal Forecasting System.

Figure 2: Study location: Point Beach State Forest, WI. A) Location of study site (marker). B) Aerial photograph of a portion of the study site showing shoreline dunes, shoreface, and nearshore bars.

Figure 3: Normalized Gaussian distribution of significant wave height at Point Beach State Forest for 2020 and the survey period (08/11/2020-09/05/2020).

Figure 4: Topo-bathymetric survey points (black markers) and interpolated 0.5 m interval contour map for the two survey dates.

Figure 5: Computation grid of XBeach model. Left is onshore, right is offshore.

Figure 6: Hydrodynamic data for the RBR*solo*^{3} pressure transducer, XBeach nearshore model outputs, and Great Lakes Coastal Forecasting System (GLCFS) node, approximately 1 km offshore. GLCFS data are color coded by angle of wave incidence (0^o to North, 90^o to East).

Figure 7: A) DEM of difference between surveys. Red denotes erosion, blue is accretion. B) Cross sectional profile in center of domain showing change along a transect, with shoreward propagation of the longshore bars.

Figure 8: A) DEM of difference between final and initial model bathymetry for the highest and lowest asymmetry/skewness factor (*facua*). As *facua* increased there was less sediment movement overall, particularly in the southern and central portion of the shoreline. B) Cross sectional profile in the center of domain showing change along a transect for the highest and lowest values of *facua*.

Fig. 1.

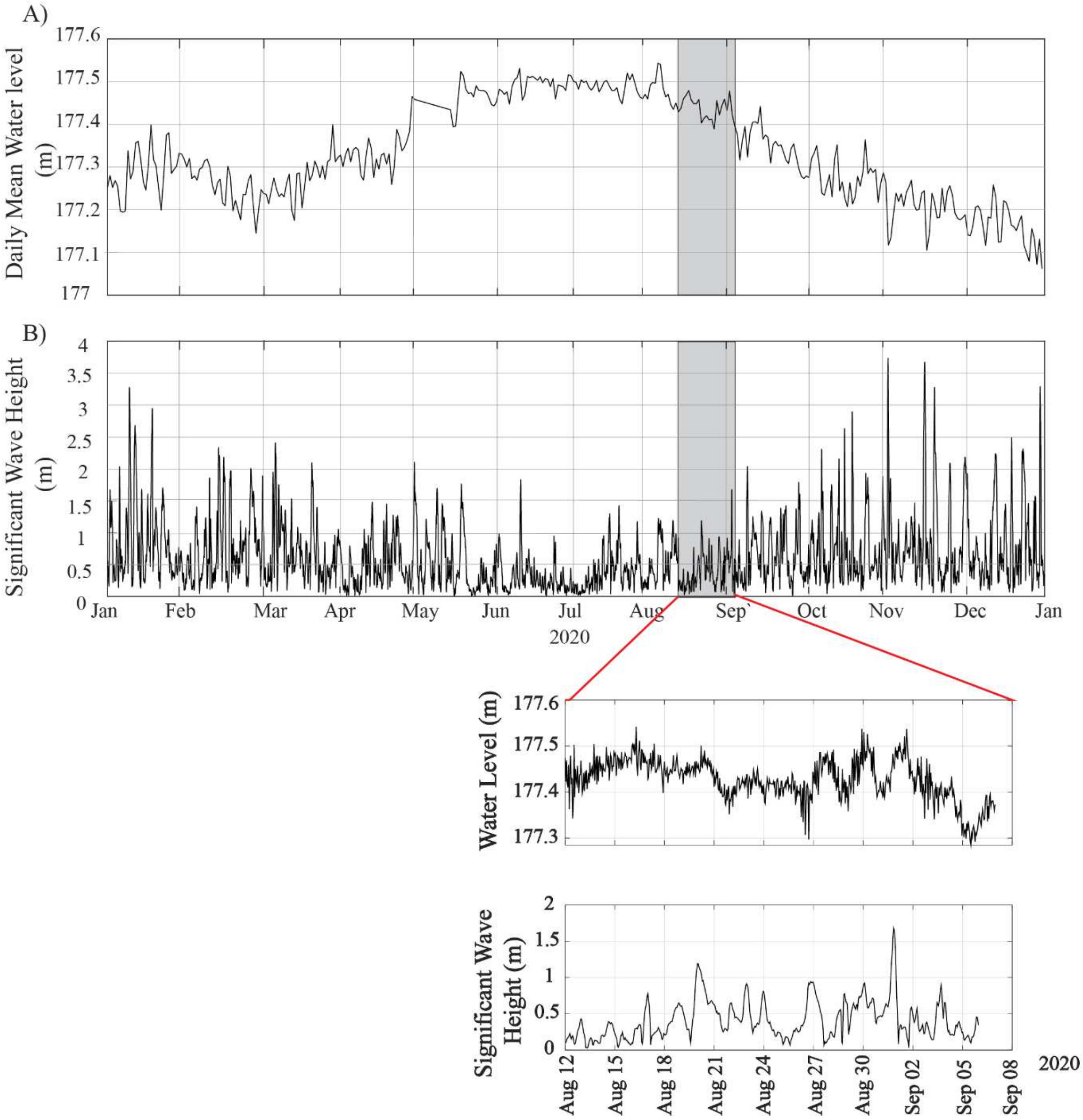

A)
Daily Mean Water level (m)
177.6
177.5
177.4
177.3
177.2
177.1
177
B)
Significant Wave Height (m)
4
3.5
3
2.5
2
1.5
1
0.5
0
Jan
Feb
Mar
Apr
May
Jun
Jul
Aug
Sep`
Oct
Nov
Dec
Jan
2020
Water Level (m)
177.6
177.5
177.4
177.3
Significant Wave Height (m)
2
1.5
1
0.5
0
Aug 12
Aug 15
Aug 18
Aug 21
Aug 24
Aug 27
Aug 30
Sep 02
Sep 05
Sep 08
2020

Fig. 2.

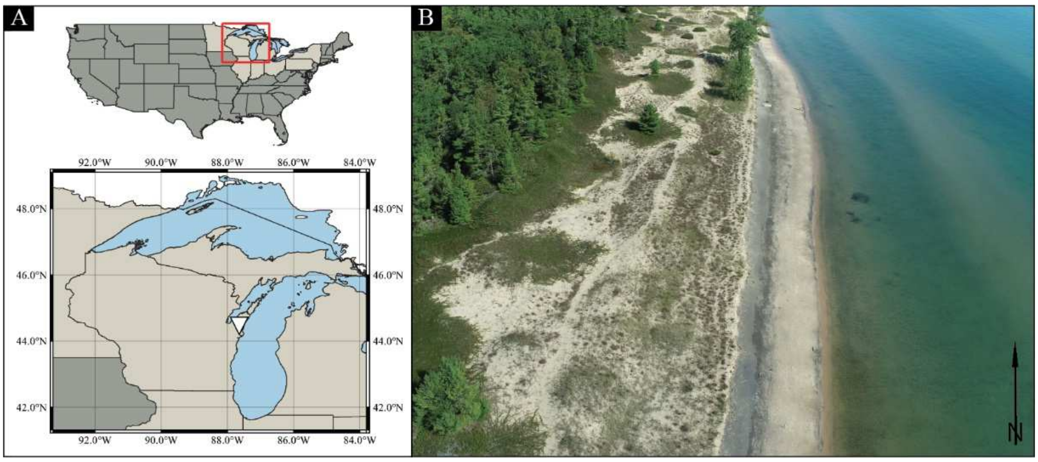

Fig. 3.

Normalized Gaussian Distribution of Wave Climate

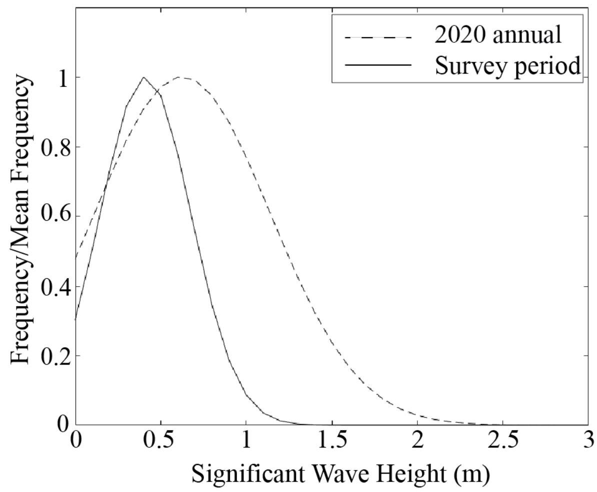

Fig. 4.

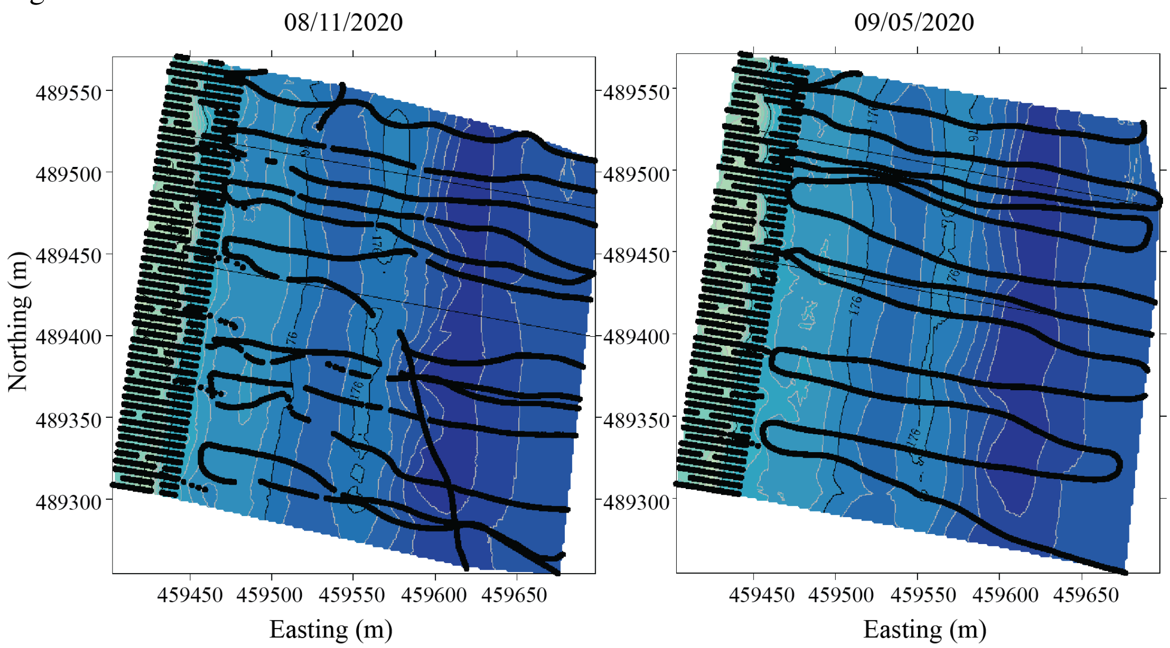

08/11/2020
09/05/2020
Northing (m)
489550
489500
489450
489400
489350
489300
459450
459500
459550
459600
459650
Easting (m)
176

Fig. 5.

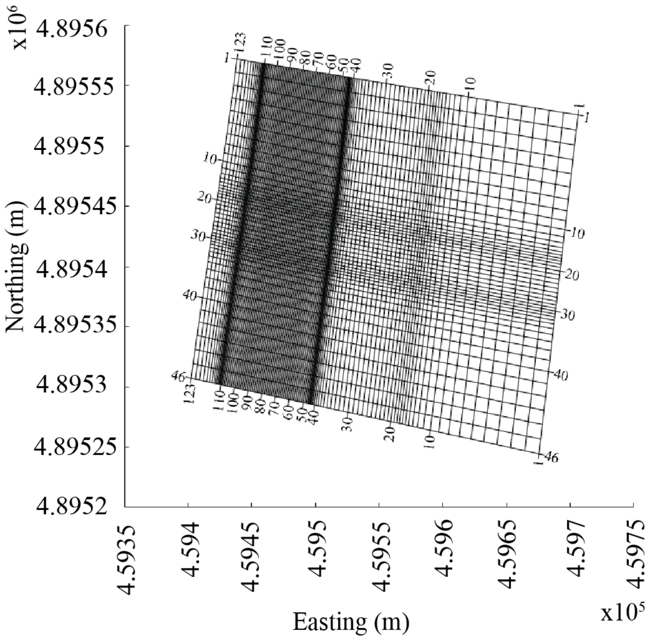

x10^6
4.8956
4.89555
4.8955
4.89545
4.8954
4.89535
4.8953
4.89525
4.8952
Northing (m)
4.5935
4.594
4.5945
4.595
4.5955
4.596
4.5965
4.597
4.5975
x10^5
Easting (m)

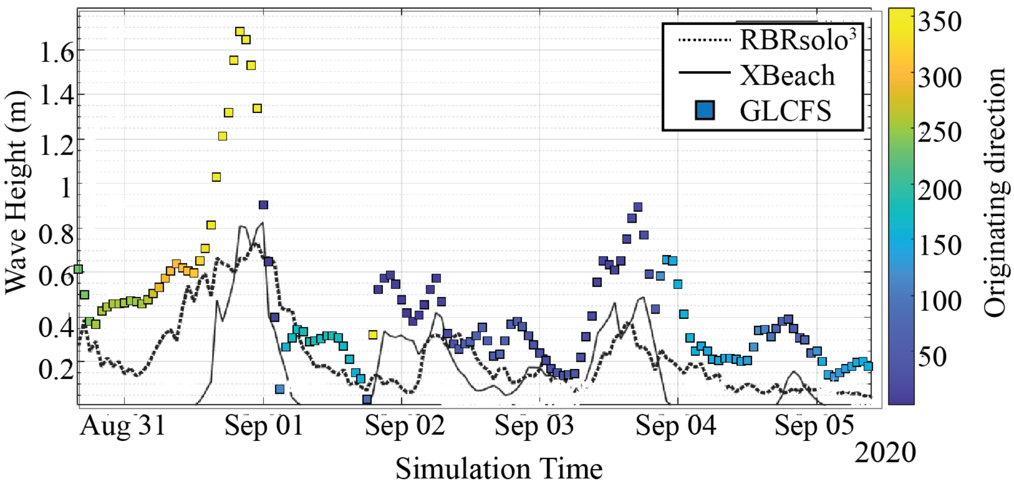
RBRsolo³
XBeach
GLCFS
Wave Height (m)
1.6
1.4
1.2
1
0.8
0.6
0.4
0.2
Aug 31
Sep 01
Sep 02
Sep 03
Sep 04
Sep 05
2020
Simulation Time
Originating direction
350
300
250
200
150
100
50

Fig. 6.

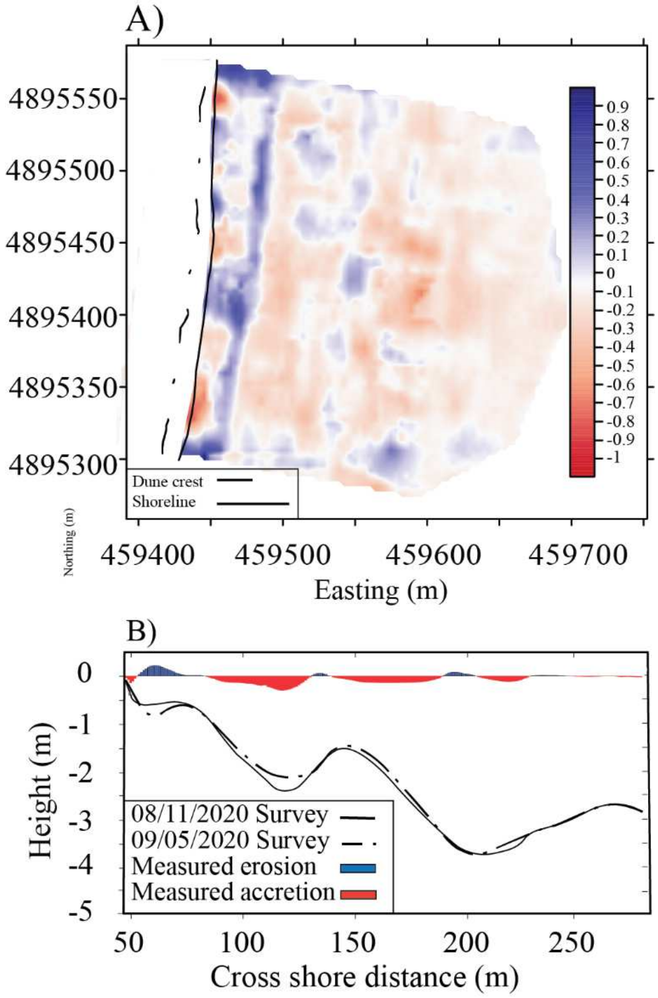

A)
4895550
4895500
4895450
4895400
4895350
4895300
Northing (m)
459400
459500
459600
459700
Easting (m)
0.9
0.8
0.7
0.6
0.5
0.4
0.3
0.2
0.1
0
-0.1
-0.2
-0.3
-0.4
-0.5
-0.6
-0.7
-0.8
-0.9
-1
Dune crest
Shoreline
B)
0
-1
-2
-3
-4
-5
Height (m)
08/11/2020 Survey
09/05/2020 Survey
Measured erosion
Measured accretion
50
100
150
200
250
Cross shore distance (m)

Fig. 7.

Fig. 8.

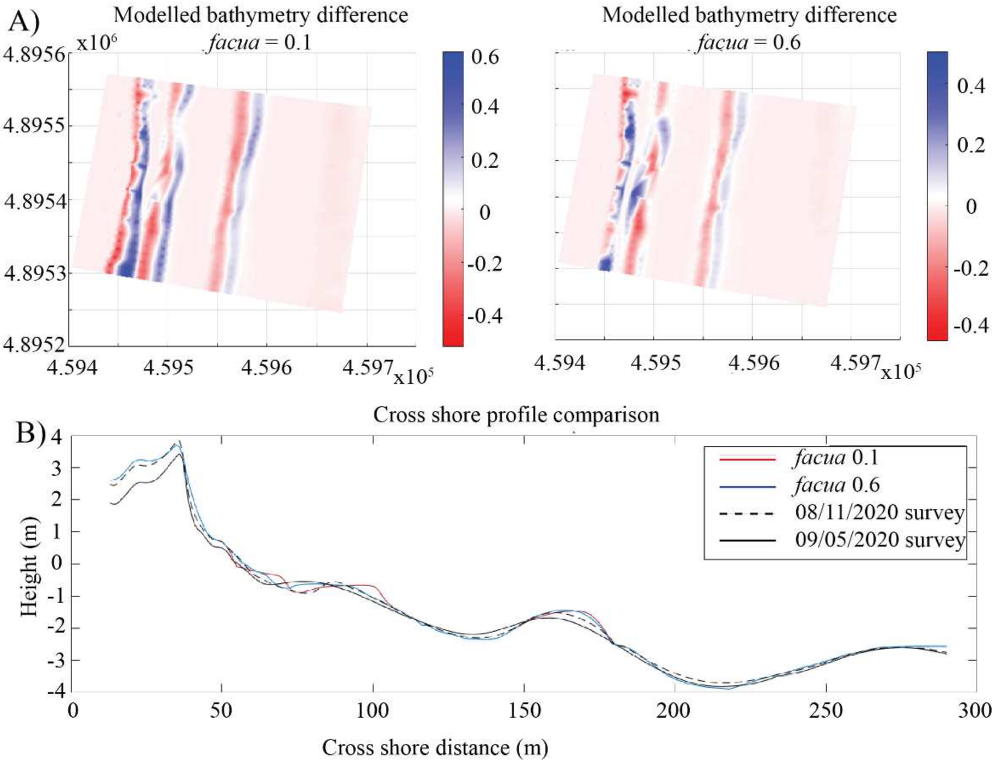

A)
Modelled bathymetry difference
facua = 0.1
x10⁶
4.8956
4.8955
4.8954
4.8953
4.8952
4.594
4.595
4.596
4.597
x10⁵
0.6
0.4
0.2
0
-0.2
-0.4
Modelled bathymetry difference
facua = 0.6
0.4
0.2
0
-0.2
-0.4
B)
Cross shore profile comparison
facua 0.1
facua 0.6
08/11/2020 survey
09/05/2020 survey
Height (m)
Cross shore distance (m)
4
3
2
1
0
-1
-2
-3
-4
0
50
100
150
200
250
300